

available at www.sciencedirect.comjournal homepage: www.elsevier.com/locate/biochempharm

L-454,560, a potent and selective PDE4 inhibitor with *in vivo* efficacy in animal models of asthma and cognition

Z. Huang^a, R. Dias^c, T. Jones^a, S. Liu^a, A. Styhler^a, D. Claveau^a, F. Otu^c, K. Ng^a, F. Laliberte^a, L. Zhang^a, P. Goetghebeur^c, W.M. Abraham^d, D. Macdonald^b, D. Dubé^b, M. Gallant^b, P. Lacombe^b, Y. Girard^b, R.N. Young^b, M.J. Turner^a, D.W. Nicholson^a, J.A. Mancini^{a,*}

^aDepartment of Biochemistry and Molecular Biology, Merck Frosst Centre for Therapeutic Research, Kirkland, Quebec, Canada

^bDepartment of Medicinal Chemistry, Merck Frosst Centre for Therapeutic Research, Kirkland, Quebec, Canada

^cDepartment of In Vivo Neuroscience, The Neuroscience Research Centre, Terlings Park, Eastwick Road, Harlow, Essex CM20 2QR, UK

^dDepartment of Research, Mount Sinai Medical Center, 4300 Alton Road, Miami Beach, FL 33140, United States

ARTICLE INFO

Article history:

Received 9 January 2007

Accepted 7 March 2007

Keywords:

Asthma

cAMP

Cognition

COPD

Inflammation

Phosphodiesterase

PDE4

ABSTRACT

Type 4 phosphodiesterases (PDE4) inhibitors are emerging therapeutics in the treatment of a number of chronic disorders including asthma, chronic obstructive pulmonary disease (COPD) and cognitive disorders. This study delineates the preclinical profile of L-454,560, which is a potent, competitive and preferential inhibitor of PDE4A, 4B, and 4D with IC_{50} values of 1.6, 0.5 and 1.2 nM, respectively. In contrast to the exclusive binding of cilomilast and the preferential binding of roflumilast to the PDE4 holoenzyme state (Mg^{2+} -bound form), L-454,560 binds to both the apo- (Mg^{2+} -free) and holoenzyme states of PDE4. The intrinsic enzyme potency for PDE4 inhibition by L-454,560 also results in an effective blockade of LPS-induced $TNF\alpha$ formation in whole blood ($IC_{50} = 161$ nM) and is comparable to the human whole blood potency of roflumilast. The cytokine profile of inhibition of L-454,560 is mainly a Th1 profile with significant inhibition of $IFN\gamma$ and no detectable inhibition of IL-13 formation up to 1 μ M. L-454,560 was also found to be efficacious in two models of airway hyper-reactivity, the ovalbumin (OVA) sensitized and challenged guinea pig and the ascaris sensitized sheep model. Furthermore, L-454,560 was also effective in improving performance in the delayed matching to position (DMTP) version of the Morris watermaze, at a dose removed from that associated with potential emesis. Therefore, L-454,560 is a novel PDE4 inhibitor with an overall *in vivo* efficacy profile at least comparable to roflumilast and clearly superior to cilomilast.

© 2007 Elsevier Inc. All rights reserved.

* Corresponding author at: Department of Biochemistry and Molecular Biology, Merck Frosst Centre for Therapeutic Research, P.O. Box 1005, Pointe Claire, Dorval, Quebec H9R 4P8, Canada. Tel.: +1 514 428 3167; fax: +1 514 428 4930.

E-mail address: joseph_mancini@merck.com (J.A. Mancini).

Abbreviations: cAMP, cyclic adenosine monophosphate; COPD, chronic obstructive pulmonary disease; CTA, conditioned taste aversion; DMTP, delayed matching to position; EAR, early airway response; FEV1, forced expiratory volume in 1 s; fMLP, f-MET-LEU-PHE; LAR, late airway response; LPS, lipopolysaccharide; LTP, long term potentiation; MED, minimal effective dose; OVA, ovalbumin; PDE, phosphodiesterase; TNF, tumor necrosis factor

0006-2952/\$ – see front matter © 2007 Elsevier Inc. All rights reserved.

doi:10.1016/j.bcp.2007.03.010

1. Introduction

Cyclic adenosine monophosphate (cAMP) is a potent second messenger with a variety of physiological and pathophysiological manifestations [1]. A few of the parameters which cAMP can modulate are smooth muscle contraction, inflammatory cell activity, mediator release, neurochemical release, and cellular adhesion. Adenylate cyclases, of which there are presently 10 human isoforms, catalyze the formation of cAMP from 5'AMP [2–5]. Since even short spikes of cAMP elevation within a cell can cause activation of several signaling pathways, the synthesis and metabolism of cAMP is tightly controlled [6]. The enzymes that metabolize cAMP to 5'AMP are termed phosphodiesterases. The phosphodiesterase gene family is comprised of 11 members of which 6 of these genes can metabolize specifically either cAMP or cGMP while the remaining 5 genes can metabolize both cAMP and cGMP [7].

Elevations of cAMP through β 2 adrenergic stimulation have been utilized extensively for the treatment of asthma and COPD [8]. The primary clinical utility for β 2 adrenergic agonists has been to cause bronchodilatation in patients with bronchial hyper-reactivity [9]. The present clinical data suggest that elevation of cAMP through β 2 adrenergic stimulation does not affect the inflammatory component of asthma or COPD [10]. In preclinical paradigms and in clinical trials, significant data have been generated that demonstrate prolonged elevation of cAMP through inhibition of PDE4 results in significant anti-inflammatory effects. Roflumilast, one of the most advanced, potent and specific PDE4 inhibitor, has been shown to decrease parenchymal lung damage and infiltration of lung macrophages in a 7-month model in mice chronically exposed to cigarette smoke [9,11]. Also, genetic mouse deletions of either PDE4B or PDE4D (two of the four orthologues of the PDE4 gene family) results in either absence of LPS induced TNF α formation from monocytes or decreased hyper-responsiveness to antigen challenge in a mouse OVA-model of airway resistance, respectively [12,13]. The most compelling data for PDE4 inhibitors is the clinical data generated with roflumilast and cilomilast. Roflumilast in a 24-week daily dosing regime of either 0.25 or 0.5 mg/day in COPD patients resulted in a statistically significant improvement in postbronchodilator FEV₁ [14]. In a clear indication of anti-inflammatory activity with PDE4 inhibitors, cilomilast dosed at 15 mg/BID for 12 weeks in COPD patients resulted in a 48 and 47% reduction in CD8⁺ and CD68⁺ cells, respectively, in lung biopsies from the inhibitor treated patients [15]. These data with cilomilast are the only published data that demonstrate decreases in airway inflammatory cells in lung tissues from COPD patients. Of the latter two compounds, only roflumilast has also demonstrated efficacy in asthma, with statistically significant improvement in FEV₁'s during the late asthmatic response in a 10-day study of allergen challenged asthmatics [16].

One of the major development hurdles for PDE4 inhibitors has been toxicity and specifically, gastrointestinal intolerance that is manifested as emesis and diarrhea. With the use of genetically manipulated mice, the data suggest that a majority of the anti-inflammatory effect of PDE4 inhibition is through PDE4B and PDE4D. The PDE4B null mice have a significantly decreased TNF α production in response to LPS and have

decreased lung inflammation in an LPS challenged model of asthma [17]. The PDE4D null mice have a decreased α 2-adrenoreceptor mediated anesthesia that is a correlate of emesis and therefore identifies PDE4D as the major isoform in the brain responsible for emesis [18]. Subtype selective PDE4 inhibitors have been a major challenge throughout the development process and recent crystallography data demonstrates that the first shell of the PDE4 active site is completely conserved between PDE4B and D [19].

Another significant indication for PDE4 inhibitors is the treatment of cognitive dysfunction. Disorders in which cognitive deficits are inherent include Alzheimer's disease, Parkinson's disease, vascular dementia, schizophrenia and stroke. Alterations in brain levels of cAMP have been linked to increases in long term potentiation (LTP) that appears critical for signaling pathways involved in cognition. Both studies with weak PDE4 selective inhibitors and PDE4D null mice have demonstrated significant increases in LTP and/or learning behavior in several assays [20–22]. The present study details effects observed with L-454,560 in the Morris watermaze in rodents and, moreover, determines a therapeutic window between memory enhancement and potential emesis.

Thus, this study describes the development of a potent and selective PDE4 inhibitor, L-454,560. This compound is a competitive and reversible PDE4 inhibitor that preferentially inhibits the hydrolysis of cAMP by PDE4A, 4B and 4D with comparable IC₅₀ values ranging from 0.5 to 1.6 nM. It is efficacious in an ovalbumin-challenged guinea pig model of airway hyper-reactivity with an ED50 of 0.03 mg/kg. L-454,560 also inhibits significantly the late asthmatic response in ascaris sensitized and challenged sheep with 95% of the LAR response inhibited at a 0.5 mg/kg IV dose. The overall profile of L-454,560 is significantly more potent than cilomilast and equivalent in human whole blood assays to the advanced clinical candidate, roflumilast. Finally, L-454,560 appears to have utility in the treatment of cognitive dysfunction by enhancing memory processes at a dose significantly lower than that found to induce conditioned taste aversion.

2. Methods and materials

2.1. Reagents

Analytical grade HEPES, EDTA, cAMP, ultra grade MgCl₂, KCl, PBS, IBMX, mepyramine, Al(OH)₃, carbachol, lithium chloride and ovalbumin reagents were purchased from Sigma/Aldrich (St. Louis, MO). [³H]-cAMP, [³H]-cGMP, and sepharose beads were purchased from GE Healthcare (Piscataway, NJ). Recombinant baculovirus proteins were prepared by the Biotechnology Research Institute (Montreal, Quebec). All products for quantitative PCR were purchased from Applied Biosystems (Foster City, CA). L-454,560 and the comparators (cilomilast and roflumilast) were synthesized by the Medicinal Chemistry Department at Merck Frosst as previously described [23].

2.2. Ethics

All procedures used in the *in vivo* assays were approved by the Animal Care Committee at the Merck Frosst Centre for

Therapeutic Research (Kirkland, Quebec, Canada) according to guidelines established by the Canadian Council on Animal Care.

2.3. PDE4A, 4B, 4C and 4D activity assays

The hydrolysis of [^3H]-cAMP or [^3H]cGMP by PDEs was monitored as previously described [31]. In order to decrease variability in PDE enzymes due to various N-terminal regulatory sequences, human PDE4A²⁴⁸ (PDE4A^{QT}) and its PDE4B, PDE4C and PDE4D equivalents were generated by creating glutathione fusion constructs in frame with the Gln-Thr (QT) located within UCR2 of the PDE4 sequences [24]. The PDE-GST constructs were expressed in SF9 cells using the baculovirus expression system and purified as GST-fusion proteins. Structurally, in addition to the removal of the inhibitory UCR1 domain of the long PDE4 variants, the PDE4QTs are comparable to the short variants (hPDE4A1, hPDE4B2, hPDE4D1 and hPDE4D2) with their putative membrane anchoring tails deleted. The PDE4 enzyme assays were conducted at a sub-saturating concentration of cAMP (0.1 μM) and a saturating concentration of Mg^{2+} -cofactor (10 mM compared with EC_{50} from 0.1 to 0.5 mM). Under these conditions, the IC_{50} values are comparable to their apparent K_i values, which are reflective of their affinities with the holoenzyme states.

2.4. Reversibility assay

GST-PDE4A^{QT} (3.5 ng) incubated at 4 °C for 10 min with L-454,560 (2 μM in DMSO) in 100 μl buffer (20 mM HEPES, pH 7.5, 1 mM EDTA, 10 mM Mg^{2+} and 100 mM KCl) was immobilized with GST-Sepharose beads (~50 μl bed volume). The PDE activity on the beads, before and after buffer washing, was detected by the addition of 190 μl of [^3H]-cAMP (0.1 μM) for 20 min at 30 °C. The activity from the immobilized PDE4/inhibitor complex after washing was compared with that from the control to determine the dissociation of the inhibitor.

2.5. PDE selectivity assays and [^3H]-rolipram binding assay

Compounds were screened against PDE1, PDE2, PDE3A, PDE3B, PDE5A, PDE6, PDE7A and PDE9A. PDE1, PDE3 and PDE7 were assayed similar to the PDE4 enzymes at 0.1 μM concentrations of cAMP. PDE5, PDE6, and PDE9 enzymes were assayed at 0.1 μM cGMP and PDE2 was assayed by MDS Pharma Services (Bothel, WA) at 1 μM cAMP. All enzymes were obtained from human recombinant sources except PDE1, which was from dog heart, PDE6 from bovine eye, and PDE2 from human platelets. The equilibrium binding affinity of compounds with PDE4A apoenzyme and holoenzyme (Mg -bound form) were determined using the non-filtration-based [^3H]-rolipram binding assay with GST-PDE4A²⁴⁸ immobilized on SPA beads as previously described [24]. The apoenzyme state was generated using 10 mM EDTA in the absence of Mg^{2+} , and the Mg^{2+} -bound holoenzyme state was generated using a saturating concentration of Mg^{2+} (6 mM) plus 1 mM EDTA to remove other advantageous divalent metal ions.

2.6. Ovalbumin-challenged model of asthma in the guinea pig

Charles River male Hartley guinea pigs were sensitized by i.p. (intraperitoneal) injection of ovalbumin (0.5 ml of a solution of 100 $\mu\text{g}/\text{ml}$ in 10% $\text{Al}_2(\text{OH})_3$). In these studies parallel groups of animals were used. Group 1 animals were pretreated with vehicle (1 ml/kg, i.p., 30 min pretreatment) while all other groups of animals in each study were pretreated with L-454,560, roflumilast or cilomilast (IP dosing in PEG200/saline, 1:1). All experiments were carried out in the presence of the H1 (histamine) receptor antagonist, mepyramine (5 mg/kg, i.p.; 30 min pretreatment). Guinea pigs were then placed individually in a whole body plethysmographic chamber that allowed the animal to move freely with minimal stress. Thirty minutes later, they were exposed to an aerosol of ovalbumin (10 mg/ml in saline) for 1 min. Changes in pulmonary parameters (Penh, Enhanced pause) were recorded for 1 h using a Buxco pulmonary mechanics analyzer model XA. Results were calculated as percent inhibition comparing the area under the curve (AUC) of the treated animal to the average AUC of the control group. All data were analyzed by applying a two-way ANOVA (Dunnett test) to the log transformed AUC's from all control and drug treatment group.

2.7. Quantitative PCR analysis of cytokine formation in whole blood

Blood from male Hartley guinea pigs or humans was utilized for ex vivo analysis of cytokine formation and inhibition as previously described [26]. Fresh blood was collected in tubes containing 0.13 M sodium citrate by cardiac puncture from isoflurane-anesthetized guinea pigs or from heparinised venous bleed of human volunteers. Briefly, 500 μl aliquots of blood were preincubated with either 2 μl of DMSO or PDE4 at 37 °C for 15 min. This was followed by incubation with 10 μl of 0.1% bovine serum albumin, 100 $\mu\text{g}/\text{ml}$ LPS (*Escherichia coli* serotype O111:B4, Sigma–Aldrich, St. Louis, MO) or concanavalin A (50 $\mu\text{g}/\text{ml}$ final) [25]. Total RNA was isolated from these samples using TRIzol reagent and then cleaned up using the RNeasy mini kit. Total RNA was reverse transcribed and cytokine mRNA levels were quantified by real time quantitative PCR.

2.8. *Ascaris* sensitized sheep model of airway resistance

A total of four sheep (24–43 kg), with airway hypersensitivity to *Ascaris suum* antigen were used. All sheep had previously been shown to develop both early (EAR) and late (LAR) airway responses and post-antigen-induced airway hyper-responsiveness (AHR) to inhaled *A. suum* antigen. The sheep were conscious and were restrained in a modified shopping cart in the prone position with their heads immobilized. For the sheep used in the airway function studies, anesthesia of the nasal passages with topical 2% lidocaine was achieved and then a balloon catheter was advanced through one nostril into the lower esophagus. The animals were intubated with a cuffed endotracheal tube through the other nostril as previously described. The Mount Sinai Medical Center Animal Research Committee is responsible for assuring the humane

care and use of experimental animals approved the procedures used in this study. Breath by breath determination of mean pulmonary airflow resistance (RL) was measured with the esophageal balloon technique described previously [27–29]. All inhibitor studies were multi-dose pretreatment studies which began before antigen challenge and experiments were performed using each sheep as its own control and treated animal. Control, vehicle and inhibitor experiments were separated by at least 14 days in order to allow a washout period for the compound or the antigen challenge. Animals were treated once daily with an IV bolus of 0.5 mg/kg of L-454,560 in PEG400/distilled water (1 ml/kg solution). On day 4, the last dose of compound or a single dose of vehicle was administered IV 2 h before an inhalation challenge with *A. suum* antigen. Baseline measurements of SRL were obtained for 30 min before vehicle or inhibitor treatment and immediately after and 1, 2, 3, 4, 5, 6, 6.5, 7, 7.5, and 8 h after antigen challenge.

2.9. Concentration response curves to carbachol aerosol

Airway responsiveness was determined from cumulative concentration response curves to carbachol inhaled as previously described with either vehicle or 4 days of pretreatment with an IV bolus of 0.5 mg/kg L-454,560 QD. RL was measured immediately after inhalation of phosphate buffered saline (PBS) and after each consecutive administration of 10 breaths of increasing concentrations of carbachol (0.25, 0.5, 1.0, 2.0 and 4.0%, w/v PBS). The provocation test was discontinued when RL increased over 400% from the post-PBS value or after the highest carbachol concentration had been administered. The cumulative carbachol concentration (in breath units [BU]) that increased RL by 400% over the post-PBS value (PC400) was calculated by interpolation from the dose–response curve. One BU was defined as one breath of a 1% (w/v) carbachol aerosol solution [27,28].

2.10. Statistical analysis

In vitro IC_{50} values were expressed as mean (\pm S.E.) of $n \geq 3$ measurements unless otherwise specified. Values in the test and figures of *in vivo* experiments are mean \pm S.E. for four sheep. Data were analyzed by one-way analysis of variance followed by Neuman–Kuels post hoc test if there was a significant overall effect. The following variables were analyzed: EAR = early airway response (maximum response immediately after challenge); LAR = peak late airway response (maximum response between 6 and 8 h post-challenge, irrespective of time) expressed as percent change from baseline; PC400 ratio = the ratio of the post-challenge/pre-challenge PC400. A ratio of 1 indicates no change in airway responsiveness, whereas a ratio below 1 indicates the development of airway hyper-responsiveness.

2.11. Rat watermaze delayed matching to position (DMTP) test

The full details of the apparatus and protocol used have been previously described [30]. In brief, male hooded Lister rats (Harlan, UK) were trained over 8 days to find a submerged

platform (10 cm diameter) in a 2 m diameter pool filled with opaque water and surrounded by visual cues. The platform position remained constant during the day but was changed from day to day, and the movements of the animals were tracked using an HVS image and software system (HVS Image Ltd., UK). Each animal received four trials per day with each trial lasting 60 s. If an animal failed to find the platform within this time, it was guided to the platform by the experimenter. The animal spent 30 s on the platform before being removed prior to its next trial. Subsequently, the effects of L-454,560 were examined on five successive test days in which rats received each day either vehicle (0.5% Methocel) or L-454,560 (0.1, 0.3 and 1.0 mg/kg) p.o. in a volume of 1 ml/kg, 30 min before trial 1 ($n = 10$ per group). During this drug testing period, the interval between trials 1 and 2 was 4 h with the inter-trial interval between trials 2–3 and 3–4 remaining at 30 s. The primary measure of recall was the difference or “savings” score between trials 1 and 2. Savings scores were calculated for each animal (averaged over five successive test days), and mean difference scores for each group were calculated. Comparisons between groups were made using ANOVA followed by Dunnett’s post hoc tests where appropriate.

2.12. Rat conditioned taste aversion test

The potential of L-454,560 to induce emesis was evaluated in the conditioned taste aversion (CTA) test. Singly housed male hooded Lister rats (Harlan, UK) were deprived of water for 22.5 h in each 24 h period for 2 days prior to two conditioning days. On each conditioning day, all rats were given 20 min access to a solution of 0.1% saccharin that has a distinct and novel flavor. The amount of this liquid consumed was recorded. Rats received either vehicle (0.5% Methocel p.o.) or L-454,560 (0.1, 0.3, 1.0 and 3.0 mg/kg p.o.) or the positive control lithium chloride (30.0 mg/kg, i.p.) in a volume of 1 ml/kg. All compounds were dosed immediately after consumption of the novel flavor ($n = 8$ per group). Subsequently, on the test day the rats were presented with the flavor again and the amount of liquid consumed was recorded. The percentage change in liquid consumption from the test session from the first conditioning day was analyzed using ANOVA, and the threshold for significance was set at $p < 0.05$. Those animals that drank less or more than twice the standard deviation away from the group mean were excluded from the study.

3. Results

3.1. PDE4 inhibitor potency and selectivity

A number of splicing variants exist for each of the four PDE4 isoforms. In order to remove the variabilities in enzyme activity and inhibitor sensitivity due to their divergent N-terminal sequences, PDE4A^{QT} (PDE4A²⁴⁸), PDE4B^{QT}, PDE4C^{QT} and PDE4D^{QT} enzymes, comprising the common region of all variants of each isoform were utilized to test PDE4 inhibitors. Functionally, the PDE4QT enzymes mimic the fully activated and PKA-phosphorylated PDE4 enzymes [24,31]. Table 1 summarizes the potency of L-454,560 (Fig. 1) at inhibiting the catalytic activities of PDE4s in comparison with cilomilast

Table 1 – Intrinsic potency of PDE4 inhibitors in enzymatic and cell based assays

Compound	IC ₅₀ values ± S.E.M. (nM) for several assays					
	PDE4AQT	PDE4BQT	PDE4CQT	PDE4DQT	HMCA (TNF α)	HWBA (TNF α)
L-454, 560	1.6 ± 0.5 (6) ^a	0.5 ± 0.1 (6)	9.1 ± 0.9 (6)	1.2 ± 0.2 (6)	17 ± 10 (8)	161 ± 23 (36)
Cilomilast	42.9 ± 1.9 (151)	40.7 ± 2.1 (150)	160 ± 8 (149)	6.9 ± 0.3 (151)	705 ± 125 (11)	18,000 ± 6100 (18)
Roflumilast	0.16 ± 0.03 (3)	0.11 ± 0.01 (4)	0.61 ± 0.05 (4)	0.11 ± 0.01 (4)	1.29 ± 0.55 (5)	140 ± 23 (15)
Roflumilast N-oxide	0.58 ± 0.03 (4)	0.37 ± 0.05 (4)	3.2 ± 0.5 (4)	0.31 ± 0.04 (4)	1.63 ± 0.65 (4)	200 ± 65 (20)

The PDE4 enzymes are constructs which express the catalytic domain of the PDE4 enzymes (QT) and have been previously described [24]. All enzyme assays were performed with 0.1 μ M CAMP as described in Section 2. Cell based assays were also utilized in which LPS stimulated production of TNF α was measured in the presence or absence of inhibitor (HWBA = human whole blood assays; HMCA = human mononuclear cell assay).

^a n, number.

and roflumilast. L-454,560 is a potent inhibitor of all four isoforms with an IC₅₀ of 1.6 nM on PDE4A. The potency of L-454,560 is within several fold that of roflumilast N-oxide (the major *in vivo* metabolite of roflumilast). Both roflumilast and L-454,560 are at least 80-fold more potent than cilomilast at inhibiting PDE4B, while they are only 5.7-fold more potent than cilomilast for inhibition of PDE4D. As shown in Fig. 2, the catalytic potency of L-454,560 decreases linearly with increasing cAMP concentrations, which demonstrates competitive inhibition, and yields an apparent K_i of 0.9 nM. When GST-PDE4A^{QT} was immobilized on to GST-Sepharose beads, the PDE4 activity on the beads was similarly inhibited by L-454,560. The bound L-454,560 dissociated rapidly from the immobilized PDE4, with over 80–90% of the PDE4 activity recovered on the beads within 5 min of buffer washing, demonstrating L-454,560 is also a rapidly reversible inhibitor. In order to demonstrate selectivity, L-454,560 was tested against other PDEs using sub-saturating concentrations of either [³H]-cAMP or [³H]cGMP as substrates accordingly. As shown in Table 2, no significant PDE activity was observed for L-454,560 for any other enzyme except for weak inhibition of PDE5 (IC₅₀ of 1 μ M). Comparing the potency for PDE5A versus the lowest potency obtained for any of the PDE4 isoforms demonstrates that L-454,560 is at least 132-fold selective for inhibition of PDE4 compared to any other PDE enzyme.

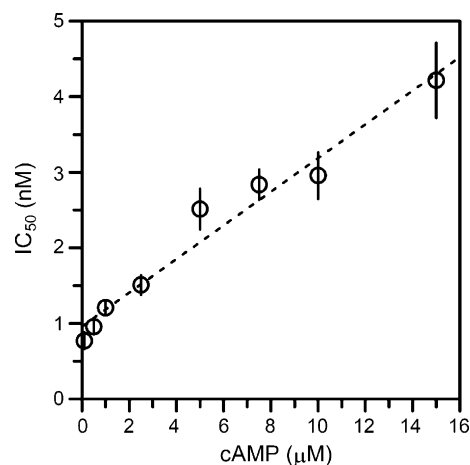


Fig. 2 – Catalytic potency and reversibility of L-454,560 for inhibition of GSTPDE4A^{QT} at increasing cAMP concentrations. Inhibition of GST-PDE4A^{QT} catalyzed hydrolysis of increased [³H]-cAMP concentration by L-454560 was monitored as detailed in methods. IC₅₀ values represent the mean (±S.E.M., n = 3). The dashed linear regression line yields an intercept (apparent K_i) at 0.9(±0.1) nM and a slope of 0.2(±0.01) nM/ μ M cAMP.

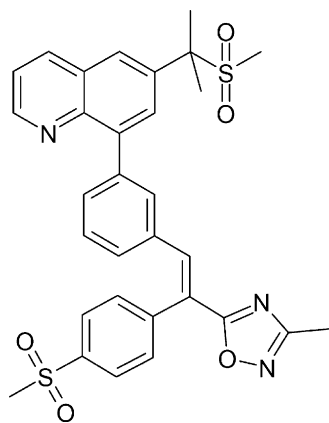


Fig. 1 – Structure of L-454,560 [6-[1-methyl-1-(methylsulfonyl)ethyl]-8-(3-{{E}}-2 (3-methyl-1,2,4-oxadiazol-5-yl)-2-[4(methylsulfonyl)phenyl]ethenyl]phenyl]quinoline].

The central PDE catalytic machinery comprises a tightly bound Zn²⁺ and a loosely bound Mg²⁺ in a binuclear motif. The reversible Mg²⁺ binding leads to the presence of two coexisting active site states (apoenzyme (Mg²⁺ free) and holoenzyme) that bind inhibitors differentially. The Mg²⁺-cofactor, with its binding affinity modulated through PKA phosphorylation [31,32] appears to be responsible for eliciting the high affinity/productive binding of cAMP and the high affinity binding of (R)-rolipram [24]. To dissect the molecular interaction of L-454560 with PDE4 further, its affinity with the two PDE4 conformers was determined using the previously described equilibrium-based [³H]-rolipram binding assay. In contrary to the exclusive binding of cilomilast reported earlier, and the preferential binding of roflumilast to the holoenzyme, L-454,560 binds to both PDE4 conformers with strong affinities (Table 3). The molecular interaction underlining this Mg-dependency for roflumilast and cilomilast has now been resolved by the identification of hydrogen bond interactions between Mg-bound waters with the pyridine nitrogen of

Table 2 – Selectivity of inhibition of L-454,560 vs. other phosphodiesterases

Phosphodiesterase	IC ₅₀	Selectivity
PDE1 (dog heart)	>10 μM	>20,000
PDE2 (rat heart)	8 μM	16,000
PDE3A (human)	27 ± 13 μM (n = 2)	>20,000
PDE3B (human)	17 ± 2 μM (n = 2)	>20,000
PDE3 (dog heart)	>10 μM	>20,000
PDE4AQT (human)	1.6 nM	2
PDE4BQT (human)	0.5 nM	1
PDE4CQT (human)	9.1 nM	18
PDE4DQT (human)	1.2 nM	2
PDE5A (human)	1.2 ± 0.3 μM (n = 6)	2,400
PDE5 a	24 μM	48,000
PDE6 (bovine)	9.8 ± 1.5 μM (n = 2)	20,000
PDE7A (human)	>10 μM	>20,000
PDE9A (human)	>20 μM	>20,000

The activities of PDE1, PDE2, PDE5, PDE6 and PDE9A were monitored using 0.1 μM of [³H]-cGMP; the activities of PDE3A/PDE3B and PDE7A were monitored using 0.01 and 0.1 μM, respectively, of [³H]-cAMP as detailed in Section 2. PDE1 and PDE2 were partially purified from dog and rat heart. PDE6 was partially purified from bovine eye. Human recombinant PDE3A and PDE3B were expressed and purified from *E. coli* [38]. Human recombinant PDE5A, PDE7A and PDE9A were expressed using a baculovirus expression system and purified from Sf9 cells.

roflumilast and with the carboxylate of cilomilast, respectively, in their PDE4 cocrystals [33].

3.2. Cytokine modulation by L-454,560 in human whole blood and mononuclear cells

The inhibition of TNFα production was utilized as a surrogate to index the cellular potency of L-454,560 in whole cells. PDE4B has been demonstrated to be induced by LPS and is responsible for the majority of the TNFα produced in monocytes. We isolated human monocytes and stimulated them with LPS in the presence or absence of a PDE4 inhibitor. Roflumilast and its N-oxide are the most potent inhibitors of TNFα production in monocytes with IC₅₀'s of 1.3 and 1.6 nM, respectively, followed by L-454,560 and cilomilast with IC₅₀'s of 17 and 705 nM, respectively (Table 1). Although roflumilast

Table 3 – Equilibrium binding affinities of inhibitors to GST-PDE4^{QT} apoenzyme and holoenzyme

Compound	Apoenzyme binding IC ₅₀ (nM)	Holoenzyme binding IC ₅₀ (nM)
L-454,560	26 ± 6 (n = 3)	6 ± 1 (n = 3)
Cilomilast	>1000	56 ± 10 (n = 6)
Roflumilast	305 ± 24	1.83 ± 0.03

The IC₅₀ values (mean ± S.E., n ≥ 3) were determined using 3 nM enzyme, 1.6 nM [³H]-rolipram, and 5 mM Mg²⁺ plus 1 mM EDTA for holoenzyme and 10 nM enzyme, 20 nM [³H]-rolipram and 10 mM EDTA for the apoenzyme, respectively, as detailed previously [24]. Under the conditions, the IC₅₀ values are reflective of their corresponding K_d values. The detection limits are ~1.5 nM for holoenzyme and 5 nM for apoenzyme from the use of 3 and 10 nM enzyme concentrations, respectively. Values for cilomilast values were reported earlier [24].

is more potent in the cell than L-454,560, a human whole blood assay, which incorporates a protein shift, and measures PDE4 dependent TNFα formation results in IC₅₀'s that demonstrate that L-454,560 and roflumilast are equipotent and both are at least 110-fold more potent than cilomilast, in this assay. The human whole blood assay has served as a biochemical readout of efficacy in several clinical trials with PDE4 inhibitors.

L-454,560 has also been more extensively profiled for its effects on several cytokines upon stimulation of human whole blood with either LPS or concanavalin A (Con A). The compounds were preincubated with the whole blood for 15 min prior to stimulation and LPS was utilized to stimulate the production of TNFα, IL-12 and GM-CSF while Con A was utilized for production of IL-2, IFNγ and IL-13. The time course production of each of these cytokines has been previously described [25] and we utilized the 4 h time point which resulted in at least 6.5-fold increase in RNA levels of each of the cytokines measured. L-454,560 is not only a potent inhibitor of TNFα, but also IFNγ, GM-CSF, IL-12 and IL-2 formation in vitro (Fig. 3). The inhibition of all these cytokines varies primarily in the extent of maximal inhibition where only TNFα and IFNγ are inhibited to 100%. We also measured IL-13 formation (data not shown) and L-454,560 did not appreciably inhibit this cytokine up to concentrations of 1 μM, suggesting a slightly more Th1 predominant inhibition profile for this class of PDE4 inhibitors similar to data obtained with a structurally distinct class of selective PDE4 inhibitors exemplified by L-826,141 [25].

3.3. Efficacy in an ovalbumin-challenged guinea pig model of asthma

Ovalbumin sensitized guinea pigs were utilized to determine the efficacy of PDE4 inhibitors against allergen-induced bronchoconstriction. In these studies, male conscious and unrestrained Hartley guinea pigs, previously sensitized to ovalbumin, were pretreated with test drug or vehicle, 30 min before antigen challenge. TNFα formation was also measured in response to LPS challenge of whole blood from sensitized guinea pigs in order to correlate the inhibition of bronchoconstriction with a pharmacodynamic whole blood surrogate of PDE4 inhibitory activity. L-454,560 produced a dose related inhibition of ovalbumin induced bronchoconstriction in conscious guinea pigs (Fig. 4A). Maximum inhibition (approximately 73–78%) was obtained in the guinea pig ovalbumin model with doses ranging from 0.1 to 0.3 mg/kg administered 30 min before antigen challenge. Plasma concentrations achieved at maximal inhibition of bronchoconstriction with these doses of L-454,560 were lower than the IC₅₀ for TNFα inhibition (see Table 4 and Fig. 4B). Roflumilast and cilomilast also produced dose dependent inhibition of antigen-induced bronchoconstriction (Table 4). The data summarized in Table 4 displays the percentage inhibition of bronchoconstriction versus plasma concentration for the three PDE4 inhibitors. These results indicate that both roflumilast and L-454,560 exhibit comparable maximum efficacy in this model (with roflumilast reaching a plateau of inhibition at 81–91%). However, maximum inhibition of bronchoconstriction was achieved at a plasma level equivalent to the guinea pig TNFα whole blood IC₅₀ for roflumilast and approaching the guinea pig TNFα whole blood IC₅₀ for L-454,560 (TNFα IC₅₀; 12 nM for

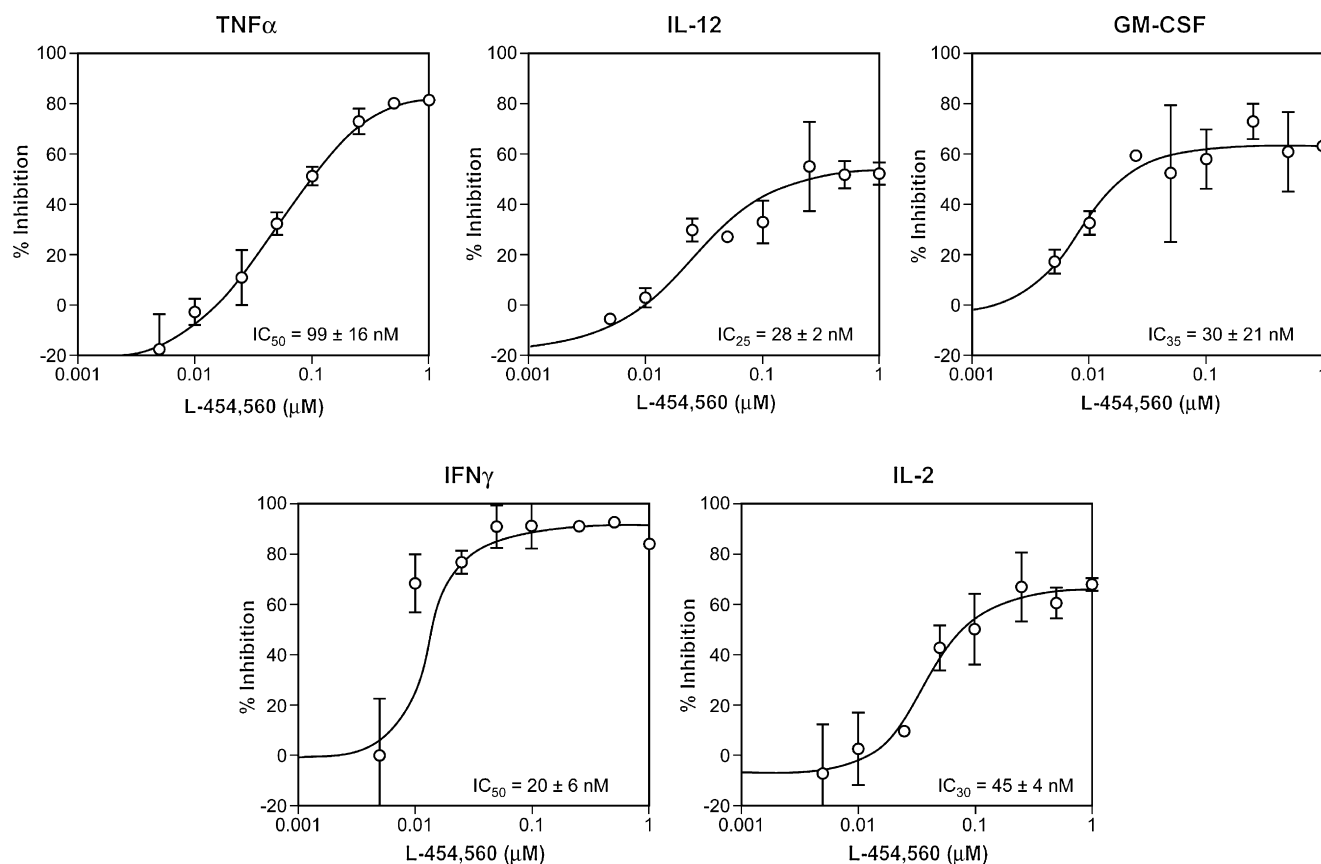


Fig. 3 – Cytokine modulation by L-454,560 in stimulated human whole blood. Heparanized whole blood was preincubated with either L-454,560 or vehicle for 15 min. After the preincubation, whole blood was challenged for 4 h with LPS for formation of TNF α , IL-12 and GM-CSF or Con A for the production of IL-2 and IFN γ . At the end of the incubation, total RNA was isolated and analyzed by real time quantitative PCR. Relative TNF α , IL-2, IL-12, GM-CSF and IFN γ levels were determined and reported as a percentage of inhibition of the vehicle control. Data are presented as the mean \pm S.E.M. of $n = 3$ experiments except for TNF α ($n = 4$).

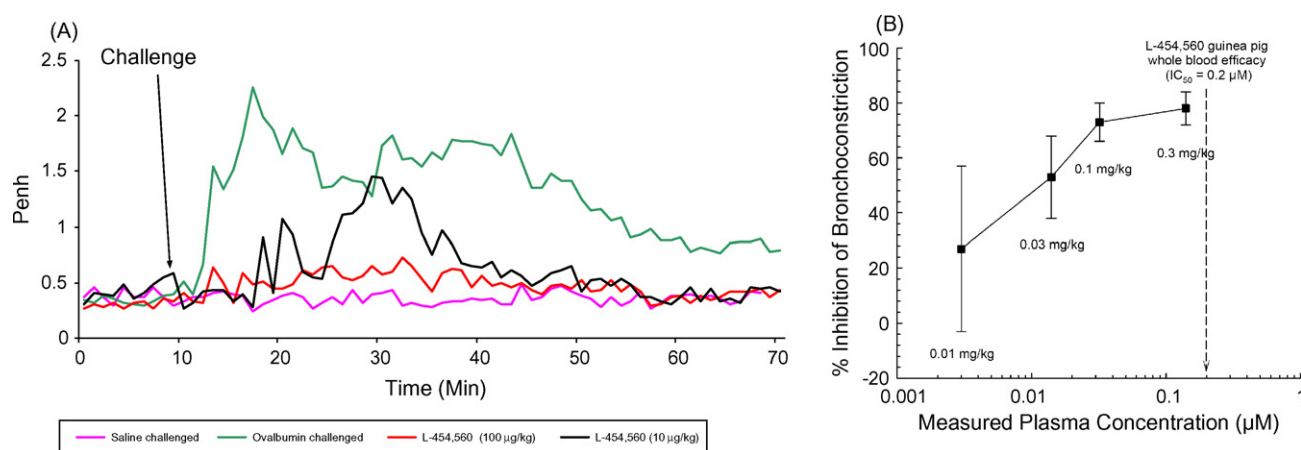


Fig. 4 – Inhibition of ovalbumin induced bronchoconstriction in guinea pigs. OVA-sensitized male Hartley guinea pigs were treated with mepyramine (5 mg/kg, i.p.) and placed in a whole body plethysmograph chamber to acclimatize. The guinea pigs were dosed i.p. with various doses of L-454,560 or a vehicle control and 30 min later challenged with aerosolized OVA (10 mg/ml in saline) or a saline vehicle for 1 min. Changes in airway resistance (PenH as a measure of bronchoconstriction) were monitored for 1 h using a Buxco pulmonary mechanics analyzer. A representative raw data set (A) is plotted as PenH measurement of individual guinea pigs dosed with either vehicle or two doses of L-454,560 (0.01 and 0.1 mg/kg, i.p.) as a function of time (measurements every 1 min). The complete data set is also plotted as % inhibition of bronchoconstriction vs. measured plasma concentration (B) at the three indicated doses of L-454,560 ($n = 4$).

Table 4 – Comparison of efficacy in guinea pig with plasma levels and potency in whole blood

Compound	Dose ($\mu\text{g}/\text{kg}$)	Efficacy % inh. broncho.	Plasma Conc. (nM)	qPCR WBA IC_{50} (nM)
Roflumilast	1	27 \pm 21 (3)	nd	10 \pm 3 (5)
	3	65 \pm 12 (4)	nd	
	10	91 \pm 10 (4)	12	
	30	81 \pm 7 (4)	42	
L-454,560	10	27 \pm 30 (4)	3	215 \pm 82 (6)
	30	53 \pm 16 (4)	14	
	100	73 \pm 7 (4)	33	
	300	78 \pm 6 (4)	140	
Cilomilast	1000	4 \pm 17 (4)	1000	420 \pm 96 (7)
	3000	64 \pm 5 (4)	2800	
	10,000	56 \pm 7 (4)	8800	

nd = not detectable; roflumilast and cilomilast along with L-454,560 were tested in the OVA challenged guinea pig model of airway resistance (Fig. 4). The results for efficacy are expressed as % inhibition of bronchoconstriction (inh. broncho.) \pm S.E.M. (number) as compared to the plasma level and the inhibition of TNF α formation in guinea pig whole blood (qPCR WBA, mean \pm S.E.M. (number of replicates)).

roflumilast versus 215 nM for L-454,560). In contrast, maximal efficacy achieved with cilomilast was only 64% and this required drug plasma levels in excess of 20-fold higher than the IC_{50} for inhibition of TNF α formation (see Table 4). These

data suggest that L-454,560 and roflumilast achieve efficacy in a guinea pig OVA-model at or below their IC_{50} for whole blood inhibition of TNF α .

3.4. Efficacy in an ascaris sensitized sheep model of airway resistance

A second pharmacological model was utilized for efficacy of PDE4 inhibitors, conscious female sheep with a naturally acquired hypersensitivity for *A. suum* antigen which develop an asthma-like bronchoconstriction upon exposure to inhaled antigen. The response in the sheep is characterized by an early (0–3 h) and late phase bronchoconstriction (4–8 h) followed 24 h later by an increase in airway hyper-reactivity. The efficacy in this model is measured as percentage change in lung resistance over time. As illustrated in Fig. 5, treatment with 0.5 mg/kg, IV of L-454,560 reduced the early airway response (EAR) to allergen but completely blocked the LAR (95% inhibition) immediately after challenge. RL returned to near baseline values by 4 h post-challenge but began to increase again by 5 h post-challenge. The peak increase in the LAR from 6 to 8 h was 151 \pm 10% over baseline. Values for the sheep post-dosing arm of the study were similar to those obtained in the pre-dosing vehicle control: EAR = 255 \pm 81% and LAR = 143 \pm 15%. When these same animals were treated with L-454,560 there was no statistically significant effect on the EAR to inhaled antigen: RL increased 153 \pm 65%. By 4 h post-challenge, however, RL had returned to baseline and increased only slightly throughout the remainder of the 8 h challenge period (peak increase in RL 17 \pm 6% ($p < 0.001$ versus vehicle and post-dosing control sheep)). L-454,560 not only blocked the LAR in these animals but also blocked the post-antigen-induced AHR. In the control trial 1 PC400 at 24 h fell to 14.5 \pm 0.3 BU from a pre-challenge value of 26.4 \pm 3.4 BU, resulting in a decreased post/pre-challenge PC400 (0.57 \pm 0.07), indicative of AHR. The data for the bracketed control (sheep control post-dose) were similar: post/pre-challenge PC400 = 0.57 \pm 0.02. When the animals were treated with L-454,560 the post/pre-challenge PC400 was 1.13 \pm 0.09 ($p < 0.001$ versus sheep vehicle and post-dose control), indicating no change in airway responsiveness, as the post-challenge PC400 (27.9 \pm 2.9 BU) was not different from the pre-challenge value of 26.4 \pm 2.9 BU (Fig. 5). Roflumilast and

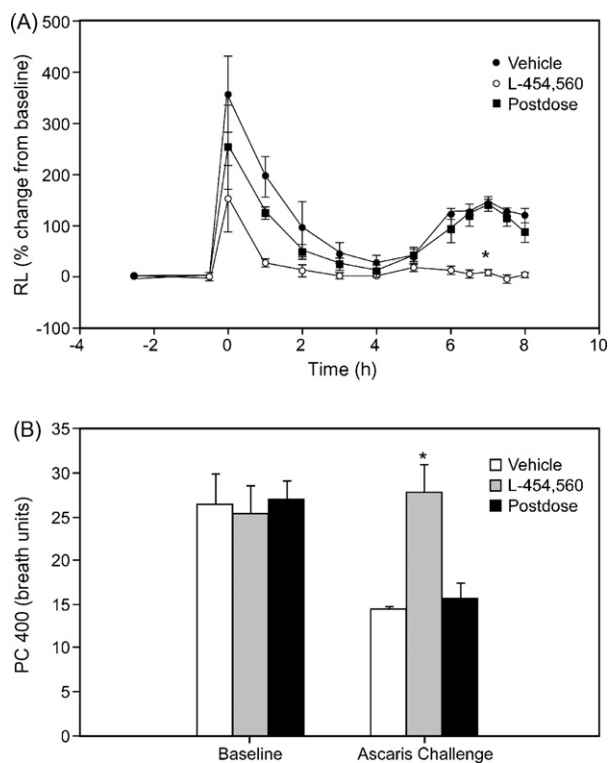


Fig. 5 – Effect of treatment with L-454,560 on the time course of antigen-induced changes in lung resistance (RL) in allergic sheep. (A). L-454,560 (0.5 mg/kg IV bolus, QD \times 4 days) partially inhibited the early airway response, but completely blocked the late airway response. The change in airway responsiveness to inhaled carbachol is also presented (B). L-454,560 completely inhibited the development of post-antigen-induced airway hyper-responsiveness (the fall in PC400). Values are mean \pm S.E. for four female sheep. * $p < 0.001$ vs. vehicle control and washout post-dose sheep.

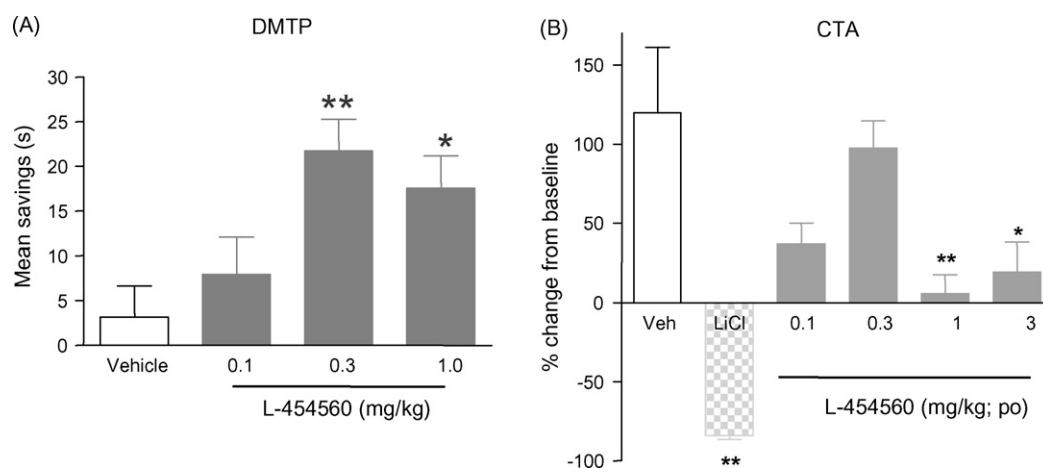


Fig. 6 – Effect of treatment with L-454,560 in the delayed match to position (DMTP) version of the Morris watermaze (A) and conditioned taste aversion (CTA) (B) tests. (A) L-454,560 produced a significant dose-dependent enhancement in performance in the DMTP watermaze as measured by the increase in savings score relative to vehicle-treated controls, with a minimal effective dose (MED) of 0.3 mg/kg. (B) L-454,560 was ineffective in the CTA assay at the DMTP watermaze MED of 0.3 mg/kg, although malaise was observed as evidenced by a significant change from baseline, at doses of 1 mg/kg and higher (data is presented as mean \pm S.E.M., ** $p < 0.01$, * $p < 0.05$).

cilomilast were also tested in this sheep model of airway resistance and both compounds displayed similar efficacy as L-454,560, the only difference was that roflumilast was dosed at 0.2 mpk/day (IV bolus \times 4 days, QD, $n = 2$). Therefore, in the sheep ascaris model, all three inhibitors demonstrated similar levels of efficacy with the majority of the efficacy occurring during the LAR.

3.5. Rat delayed matching to position (DMTP) watermaze test

cAMP is a key second messenger that plays a major role in long term potentiation and appears to be a significant regulator of cognitive function. Utilizing L-454,560, we have tested the role of this selective PDE4 inhibitor in a rodent model of cognition, the delayed matching to position (DMTP) watermaze test of spatial memory. ANOVA revealed a main effect of treatment ($p < 0.05$) and post hoc tests showed that L-454,560 at a dose of both 0.3 and 1.0 mg/kg significantly increased the mean savings score between several experiments compared to vehicle-treated controls ($p < 0.01$ and $p < 0.05$, respectively) (Fig. 6A). There was no effect of treatment on mean swim speeds averaged over the 5 days of treatment [$F < 1$]. The increased mean savings score suggests that L-454,560 resulted in an enhancement in memory in locating the submerged platform in the watermaze after conditioned testing.

3.6. Rat conditioned taste aversion (CTA) test

Since PDE4 inhibitors have a potential for gastrointestinal adverse events, L-454,560 was tested in a rat CTA experiment. This experiment was performed in order to determine the window between efficacy in DMTP and malaise in CTA. As seen in Fig. 6B, the 0.3 mg/kg dose effective in DMTP had no effect on CTA, but doses of either 1 or 3 mg/kg, like lithium, were significantly changed from the vehicle-treated controls

in the CTA model ($p < 0.05$). This data demonstrates that L-454,560 has a maximal window of three-fold for efficacy in DMTP as compared to adverse events demonstrated by CTA.

3.7. CNS mediated cAMP elevation with L-455,560

Using ICV cannulation and a dialysate, cAMP elevation in the CSF fluid of rats dosed orally with L-454,560 was monitored. Dosing of 1 mg/kg of L-454,560 in an unchallenged rat resulted in no significant elevation of cAMP compared to vehicle control treated rats. When 20 mM IBMX was added to the perfusate of rats dosed with 1 mg/kg of L-454,560, a $46.7 \pm 10.2\%$ increase in cAMP was detectable as compared to vehicle dosed rats. This suggests that an initial burst of cAMP may be required in order to detect global CNS changes in cAMP mediated by L-454,560.

Overall this data further supports a role for cAMP elevating agents playing a role in cognitive enhancement.

4. Discussion and conclusions

This study demonstrates that L-454,560 is a potent, selective and reversible inhibitor of PDE4. L-454,560 is a low nM inhibitor of all four of the PDE4 enzyme isoforms, and the compound is shifted about 300-fold ($IC_{50} = 160$ nM) with respect to the TNF α surrogate of inhibition in human whole blood. Based on the PDE enzymes tested, L-454,560 is at least 132-fold selective for inhibition of PDE4 over the other eight PDE gene families tested. L-454,560 is unique amongst the three compounds profiled in that it binds to both the apo- and holoenzyme of PDE4 with similar potency while both roflumilast and cilomilast preferentially inhibit the holoenzyme over the apoenzyme. Since the in vitro Mg^{2+} binding affinity is regulated by the PKA-mediated Ser⁵⁴ phosphorylation [31,32], it would be interesting to further evaluate whether

the dual binding of L-454,560 to the coexisting apo- and holoenzyme conformers alters the temporal regulation features of the cAMP-mediated signaling in comparison to those compounds that selectively target the holoenzyme population. L-454,560 inhibits TNF α , IFN γ , GM-CSF, IL-2 and IL-12 formation while sparing IL-13 formation in stimulated whole blood. This suggests that PDE4 inhibitors have a slightly more Th1 skewed profile of inhibition rather than Th2.

L-454,560 is also very efficacious in several animal models of airway inflammation. In an ovalbumin sensitized and challenged model of airway resistance, L-454,560 significantly reversed the bronchoconstriction obtained in guinea pigs after a single dose of 0.1 mg/kg, i.p. Roflumilast was also efficacious in this guinea pig model with maximal efficacy achieved at a dose of 0.01 mg/kg, i.p. The difference in doses required for these two compounds can be mainly attributed to the fact that roflumilast is 21-fold more potent in the guinea pig than L-454,560 (TNF α IC₅₀ = 10 \pm 3 nM for roflumilast as compared to IC₅₀ = 215 \pm 82 nM for L-454,560). Interestingly, we also tracked the blood exposure in the guinea pig and at maximal efficacious doses L-454,560 reached levels that were only 0.15 \times the IC₅₀ for inhibition of TNF α formation by L-454,560 and roflumilast was approximately at the IC₅₀ for maximal inhibition of bronchoconstriction. These data suggest that complete inhibition of the TNF α surrogate is not required to obtain significant therapeutic efficacy in this guinea pig model of airway resistance. These data also demonstrate that PDE4 inhibitors are efficacious in an acute model of lung resistance and might provide smooth muscle relaxation in acute asthma. This has also been delineated in the PDE4D null mice which have a significantly decrease airway smooth muscle cell contractility [34]. Although smooth muscle relaxation appears robust in these animal models it is not as evident in human asthma since roflumilast has been shown to have a more prominent effect on the late asthmatic response in humans [35] as compared to the early asthmatic response, of which the latter would indicate direct effects on smooth muscle contractility.

L-454,560 also demonstrated efficacy in an ascaris sensitized and challenged sheep model of asthma. In this sheep model, the major efficacy obtained is in the LAR, similar to roflumilast's efficacy in humans and in decreasing bronchial hyper-reactivity. Therefore, these data suggest that L-454,560 has more significant effects on the inflammatory component of allergic asthma than direct bronchodilatory effects on smooth muscle contractility. The sheep model is a reasonable surrogate for human asthma since there exists an early bronchoconstrictive phase that is mainly due to smooth muscle contraction, and a LAR that is associated with the secretion of inflammatory mediators such as cytokines, chemokines, and leukotrienes. Roflumilast in an allergen challenged paradigm in humans demonstrated a 28% reduction in FEV₁ changes in the EAR and 43% reduction in FEV₁ changes in the LAR [35]. Therefore both the sheep and human data suggest that the major effects of PDE4 inhibitors on clinical symptoms of asthma are related to the anti-inflammatory properties of these compounds.

PDE4 inhibitors have demonstrated human clinical efficacy in asthma and COPD but may be limited due to dose related adverse gastrointestinal events. The efficacy achieved in the

watermaze DMTP task and the profile of L-454,560 suggests that these compounds may provide benefit in cognitive impairment for the treatment of disorders such as Alzheimer's disease. One potential issue with the DMTP data is the disconnect with the lack of elevation of brain levels of cAMP with L-454,560 in normal rats dosed with this compound. This might be explained by the fact that these rats were unchallenged and the watermaze experiments may have generated a cAMP spike which would be enhanced with L-454,560 treatment. Our data with L-454,560 are also consistent with data generated with rolipram demonstrating restoration of LTP in a transgenic mouse model of Alzheimer's disease [36]. Utilizing mice with either PDE4B or PDE4D deleted has also demonstrated that the PDE4D knockout mice have improved long term memory in the Morris watermaze and radial arm maze tests of cognition [37]. Since highly selective PDE4D inhibitors have been difficult to develop and PDE4D appears to be involved in the toxicity associated with emesis [18], a clinical therapeutic window will have to be established with compounds having profiles such as L-454,560. The next few years shall demonstrate if these PDE4 inhibitors shall have significant clinical efficacy in the treatment of cognitive disorders in addition to their demonstrated efficacy in asthma and COPD.

REFERENCES

- [1] Barnes PJ. Beta-adrenoceptors on smooth muscle, nerves and inflammatory cells. *Life Sci* 1993;52:2101-9.
- [2] Cooper DM, Mons N, Karpen JW. Adenylyl cyclases and the interaction between calcium and cAMP signalling. *Nature* 1995;374:421-4.
- [3] Iyengar R. Molecular and functional diversity of mammalian Gs-stimulated adenylyl cyclases. *FASEB J* 1993;7:768-75.
- [4] Sunahara RK, Dessauer CW, Gilman AG. Complexity and diversity of mammalian adenylyl cyclases. *Annu Rev Pharmacol Toxicol* 1996;36:461-80.
- [5] Taussig R, Gilman AG. Mammalian membrane-bound adenylyl cyclases. *J Biol Chem* 1995;270:1-4.
- [6] Houslay MD, Milligan G. Tailoring cAMP-signalling responses through isoform multiplicity. *Trends Biochem Sci* 1997;22:217-24.
- [7] Lugnier C. Cyclic nucleotide phosphodiesterase (PDE) superfamily: a new target for the development of specific therapeutic agents. *Pharmacol Ther* 2006;109:366-98.
- [8] DeGraff Jr AC, Bouhuys A. Mechanics of air flow in airway obstruction. *Annu Rev Med* 1973;24:111-34.
- [9] Fitzpatrick MF, Mackay T, Driver H, Douglas NJ. Salmeterol in nocturnal asthma: a double blind, placebo controlled trial of a long acting inhaled beta 2 agonist. *BMJ* 1990;301:1365-8.
- [10] Rogers DF. Mucociliary dysfunction in COPD: effect of current pharmacotherapeutic options. *Pulm Pharmacol Ther* 2005;18:1-8.
- [11] Martorana PA, Beume R, Lucattelli M, Wollin L, Lungarella G. Roflumilast fully prevents emphysema in mice chronically exposed to cigarette smoke. *Am J Respir Crit Care Med* 2005;172:848-53.
- [12] Jin SL, Conti M. Induction of the cyclic nucleotide phosphodiesterase PDE4B is essential for LPS-activated TNF-alpha responses. *Proc Natl Acad Sci USA* 2002;99:7628-33.

- [13] Hansen G, Jin S, Umetsu DT, Conti M. Absence of muscarinic cholinergic airway responses in mice deficient in the cyclic nucleotide phosphodiesterase PDE4D. *Proc Natl Acad Sci USA* 2000;97:6751–6.
- [14] Rabe KF, Bateman ED, O'Donnell D, Witte S, Bredenkroder D, Bethke TD. Roflumilast—an oral anti-inflammatory treatment for chronic obstructive pulmonary disease: a randomised controlled trial. *Lancet* 2005;366:563–71.
- [15] Gamble E, Grootendorst DC, Brightling CE, Troy S, Qiu Y, Zhu J, et al. Antiinflammatory effects of the phosphodiesterase-4 inhibitor cilomilast (Arimflo) in chronic obstructive pulmonary disease. *Am J Respir Crit Care Med* 2003;168:976–82.
- [16] Nell H, Louw C, Leichtl S, Rathgeb F, Neuhäuser M, Bardin PG. Acute anti-inflammatory effect of the novel phosphodiesterase 4 inhibitor roflumilast on allergen challenge in asthmatics after a single dose. *Am J Respir Crit Care Med* 2000;161:A200.
- [17] Ariga M, Neitzert B, Nakae S, Mottin G, Bertrand C, Pruniaux MP, et al. Nonredundant function of phosphodiesterases 4D and 4B in neutrophil recruitment to the site of inflammation. *J Immunol* 2004;173:7531–8.
- [18] Robichaud A, Stamatou PB, Jin SL, Lachance N, Macdonald D, Laliberte F, et al. Deletion of phosphodiesterase 4D in mice shortens alpha(2)-adrenoceptor-mediated anesthesia, a behavioral correlate of emesis. *J Clin Invest* 2002;110:1045–52.
- [19] Van Der MM, Boss H, Couwenberg D, Hatzelmann A, Sterk GJ, Goubitz K, et al. Novel selective phosphodiesterase (PDE4) inhibitors. 4. Resolution, absolute configuration, and PDE4 inhibitory activity of cis-tetra- and cis-hexahydrophthalazinones. *J Med Chem* 2002;45:2526–33.
- [20] Navakkode S, Sajikumar S, Frey JU. Mitogen-activated protein kinase-mediated reinforcement of hippocampal early long-term depression by the type IV-specific phosphodiesterase inhibitor rolipram and its effect on synaptic tagging. *J Neurosci* 2005;25:10664–70.
- [21] Zhang HT, O'Donnell JM. Effects of rolipram on scopolamine-induced impairment of working and reference memory in the radial-arm maze tests in rats. *Psychopharmacology* 2000;150:311–6.
- [22] Zhang HT, Huang Y, Suvana NU, Deng C, Crissman AM, Hopper AT, et al. Effects of the novel PDE4 inhibitors MEM1018 and MEM1091 on memory in the radial-arm maze and inhibitory avoidance tests in rats. *Psychopharmacology* 2005;179:613–9.
- [23] Macdonald D, Mastracchio A, Perier H, Dube D, Gallant M, Lacombe P, et al. Discovery of a substituted 8-arylquinoline series of PDE4 inhibitors: Structure-activity relationship, optimization, and identification of a highly potent, well tolerated PDE4 inhibitor. *Bioorg Med Chem Lett* 2005;15:5241–6.
- [24] Liu S, Laliberte F, Bobechno B, Lario P, Gorseth E, Van Hamme J, et al. Dissecting the cofactor-dependent and independent bindings of PDE4 inhibitors. *Biochemistry* 2001;40:10179–86.
- [25] Claveau D, Chen SL, O'Keefe S, Zaller DM, Styhler A, Liu S, et al. Preferential inhibition of T Helper 1, but not T Helper 2, cytokines in vitro by L-826,141 [2-{3,4-bis-difluoromethoxyphenyl}-2-[4-{1,1,1,3,3,3-hexafluoro-2-hydroxypropan-2-yl)-phenyl]-ethyl}-3-methylpyridine-1-oxide], a potent and selective phosphodiesterase 4 inhibitor. *J Pharmacol Exp Ther* 2004;310:752–60.
- [26] Muise ES, Chute IC, Claveau D, Masson P, Boulet L, Tkalec L, et al. Comparison of inhibition of ovalbumin-induced bronchoconstriction in guinea pigs and in vitro inhibition of tumor necrosis factor-alpha formation with phosphodiesterase 4 (PDE4) selective inhibitors. *Biochem Pharmacol* 2002;63:1527–35.
- [27] Abraham WM, Ahmed A, Sabater JR, Lauredo IT, Botvinnikova Y, Bjercke RJ, et al. Selectin blockade prevents antigen-induced late bronchial responses and airway hyper-responsiveness in allergic sheep. *Am J Respir Crit Care Med* 1999;159:1205–14.
- [28] Abraham WM, Gill A, Ahmed A, Sielczak MW, Lauredo IT, Botvinnikova Y, et al. A small-molecule, tight binding inhibitor of the integrin alpha(4)beta(1) blocks antigen-induced airway responses and inflammation in experimental asthma in sheep. *Am J Respir Crit Care Med* 2000;162:603–11.
- [29] Abraham WM, Laufer S, Tries S. The effects of ML 3000 on antigen-induced responses in sheep. *Pulm Pharmacol Ther* 1997;10:167–73.
- [30] Attack JR, Bayley PJ, Seabrook JR, Wafford KA, McKernan KM, Dawson GR. L-655,708 enhances cognition in rats but is not proconvulsant at a dose selective for alpha5-containing GABAA receptors. *Neuropharmacology* 2006;51:1023–9.
- [31] Laliberte F, Han Y, Govindarajan A, Giroux A, Liu S, Bobechno B, et al. Conformational difference between PDE4 apoenzyme and holoenzyme. *Biochemistry* 2000;39:6449–58.
- [32] Sette C, Conti M. Phosphorylation and activation of a cAMP-specific phosphodiesterase by the cAMP-dependent protein kinase. Involvement of serine 54 in the enzyme activation. *J Biol Chem* 1996;271:16526–34.
- [33] Card GL, England BP, Suzuki Y, Fong D, Powell B, Lee B, et al. Structural basis for the activity of drugs that inhibit phosphodiesterases. *Structure* 2004;12:2233–47.
- [34] Mehats C, Jin SL, Wahlstrom J, Law E, Umetsu DT, Conti M. PDE4D plays a critical role in the control of airway smooth muscle contraction. *FASEB J* 2003;17:1831–41.
- [35] van Schalkwyk E, Strydom K, Williams Z, Venter L, Leichtl S, Schmid-Wirlitsch C, et al. Roflumilast, an oral, once-daily phosphodiesterase 4 inhibitor, attenuates allergen-induced asthmatic reactions. *J Allergy Clin Immunol* 2005;116:292–8.
- [36] Gong B, Vitolo OV, Trinchese F, Liu S, Shelanski M, Arancio O. Persistent improvement in synaptic and cognitive functions in an Alzheimer mouse model after rolipram treatment. *J Clin Invest* 2004;114:1624–34.
- [37] Zhang HT, Huang Y, Jin CSL, Frith SA, Zhao Y, Suvana N, et al. In: Proceedings of the 33rd annual meeting of society for neuroscience; 2003.
- [38] Scapin G, Patel SB, Chung C, Varnerin JP, Edmondson SD, Mastracchio A, et al. Crystal structure of human phosphodiesterase 3B: atomic basis for substrate and inhibitor specificity. *Biochemistry* 2004;43:6091–100.